Proteomic Profiling of Infiltrating Ductal Carcinoma Reveals Increased Cellular Interactions with Tissue Microenvironment

ARTICLE *in* JOURNAL OF PROTEOME RESEARCH · FEBRUARY 2012

Impact Factor: 4.25 · DOI: 10.1021/pr201018y · Source: PubMed

Journal of proteome research

Article

pubs.acs.org/jpr

Proteomic Profiling of Infiltrating Ductal Carcinoma Reveals Increased Cellular Interactions with Tissue Microenvironment

Michael Gormley, Alimatou Tchafa, Rong Meng, Zhijiu Zhong, and Andrew A. Quong*

Department of Cancer Biology, Kimmel Cancer Center, Thomas Jefferson University, 233 South 10th Street, Philadelphia, Pennsylvania 19107, United States

Supporting Information

ABSTRACT: Progression of invasive carcinoma involves the deregulation of molecular signaling pathways that results in the acquisition of oncogenic phenotypes. Functional enrichment analysis allows for the identification of deregulated pathways from omics scale expression data. Given the importance of post-transcriptional regulatory mechanisms on protein expression and function, identification of deregulated pathways on the basis of protein expression data is likely to provide new insights. In this study, we have developed methods for label-based mass spectrometry in a large number of samples and applied these methods toward identification and quantification of protein expression in samples of infiltrating ductal carcinoma, benign breast growths, and normal adjacent tissue. We identified 265 proteins with differential expression patterns in infiltrating ductal carcinoma relative to benign growths or normal breast tissue. Analysis of the differentially expressed proteins indicated the deregulation of signaling pathways related to proliferation, invasion and metastasis, and immune response. Our approach provides complementary information to gene expression microarray data and identifies a number of deregulated molecular signaling pathways indicative of breast cancer progression that may enable more accurate, biologically relevant diagnoses and provide a stepping stone to personalized treatment.

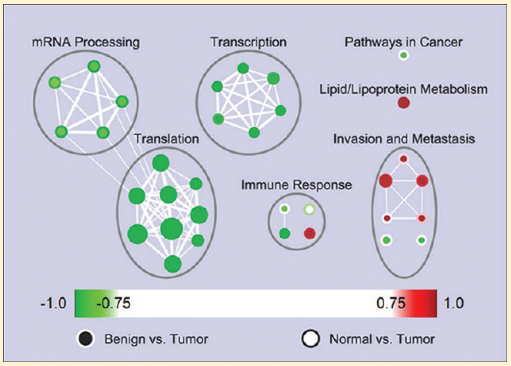

KEYWORDS: *infiltrating ductal carcinoma, quantitative label-based 2D-LC–MS/MS, pathway analysis*

INTRODUCTION

Breast cancer progression is characterized by the accumulation of mutations that lead to the deregulation of molecular signaling pathways and the acquisition of oncogenic phenotypes such as increased proliferation, insensitivity to cell death signals, and cell motility and invasion. For example, constitutive activation of the RAS oncogenes can induce increased proliferation and cell motility and inhibition of apoptosis through activation of the MAPK and PI3K pathways.[1,2] Signaling pathways downstream from RAS and other canonical oncogenes have been studied extensively; however, the functional implications of these genetic alterations have not been completely described. Additionally, individual breast tumors can carry as many as 90 mutant genes[3] with 20 or more driver mutations which contribute directly to tumorigenesis. Analysis of data from next-generation sequencing platforms will likely identify a new cohort of genomic alterations in breast cancer.[4,5] Each of these mutations is likely to have myriad effects on cellular function through modification of signal transduction in the interconnected network of molecular signaling molecules. In this setting, characterization of deregulated pathways based on genome-wide expression analysis may have clinical impact through the generation of biologically relevant classification schemes[6] and the development of novel targeted therapies to inhibit oncogenic processes and restore physiological function.

Breast cancer has been studied extensively on the basis of gene expression profiling. Clustering analysis has been applied to identify a number of molecular subtypes of disease associated with hormone receptor status, amplification of the HER2 growth factor receptor and clinical outcome.[6,7] Analysis of each of these molecular subtypes has revealed characteristic patterns of pathway deregulation.[8] In particular, basal subtypes of tumors are characterized by low estrogen receptor and progesterone receptor activation and high activation of MYC and RAS pathways.[8] These studies have provided important contributions to our understanding of the molecular heterogeneity of breast cancer; however, signal transduction in molecular signaling pathways is dependent on post-translational regulatory mechanisms, such as protein synthesis and degradation, protein–protein interactions, and modifications such as phosphorylation and acetylation. With this in mind, we profiled tissues from a large cohort of breast cancer using protein expression profiling to gain new insight into the molecular etiology of breast cancer.

The relative complexity of protein biochemistry makes the identification and quantification of proteins more challenging than gene expression profiling. Identification of proteins from complex biological samples is dependent on the accurate

Received: October 12, 2011
Published: February 22, 2012

dx.doi.org/10.1021/pr201018y | J. Proteome Res. 2012, 11, 2236–2246

measurement of the masses of peptide fragments associated with amino acid residues. The most commonly used technique compares observed mass spectra from peptide fragments to theoretical spectra generated from protein sequence databases.[9] In expression profiling, chromatographic fractionation is necessary prior to mass spectrometry to increase the number of proteins that can be detected.[10] This greatly increases the effective sample size and analysis time. Quantification of proteins can be facilitated by the use of chemical or metabolic tags.[11,12] The iTRAQ isobaric tags[12] label the n-terminus and lysine residues of peptide fragments. Each tag consists of a protein reactive group and a mass tag which includes a mass balance group and a reporter group of unique mass between 113 and 121 Da. Differentially labeled peptides coelute from chromatography columns and are detected simultaneously in the mass spectrometer. Upon peptide fragmentation, the reporter group breaks off from the mass tag such that quantification of the peptide in each sample can be determined by the intensity of the reporter ion peaks. This allows for multiplexed quantification of protein expression in up to eight samples, and increasing throughput 7-fold. Identification and quantification of proteins by label-based two-dimensional liquid chromatography tandem mass spectrometry (2D-LC−MS/MS) enables expression profiling of hundreds to thousands of proteins from complex biological samples.

Identification of molecular signaling pathways that are deregulated in the progression of breast cancer enables systematic characterization of oncogenic processes. In this study, we have developed a methodology for protein expression profiling from large sets of frozen tissue samples based on label-based quantitative 2D-LC−MS/MS and applied this methodology for protein expression profiling of infiltrating ductal carcinoma (IDC). Functional enrichment analysis indicated the deregulation of molecular signaling pathways related to proliferation, invasion and metastasis and the immune response in carcinoma compared to benign or normal adjacent tissue. These findings suggest novel hypotheses for mechanisms of tumorigenesis in breast cancer that may have important implications in diagnosis and drug development.

EXPERIMENTAL SECTION

Tissue Procurement

All samples were obtained from breast tumor tissue bank at the Kimmel Cancer Center through a protocol approved by the Institutional Review Board of Thomas Jefferson University. Samples were classified according to histology analysis. Samples were characterized as infiltrating ductal carcinoma if they exhibited signs of local tissue invasion. A total of 90 tissue samples, including 30 benign breast growths (median age 61.0 years), 34 normal adjacent to tumor (median age 66.0 years), and 26 infiltrating ductal carcinoma (median age 59.5 years) samples were selected.

Sample Preparation

Frozen tissue blocks were embedded in tissue freezing medium (Triangle Biomedical Sciences). From each block, 20 μm slices of tissue were sectioned and washed extensively with PBS. Protein was extracted by heating in lysis buffer (4% sodium dodecyl sulfate (SDS), 100 mM TEAB, 20 mM DTT) at 90 °C for 10 min. Samples were cooled to room temperature, sonicated for 10 cycles and spun at 14000× g for 10 min. The supernatant from each sample was collected and diluted 4× to eliminate interference from DTT and allow for protein quantification using the bicinchoninic acid (BCA) assay (Thermo Scientific). A 29 μg aliquot of proteins was collected from each sample and reduced, alkylated and trypsin digested using the filtration-aided sample processing (FASP) procedure described by Mann et al.[13] in a 96-well filter plate format (Millipore). The FASP protocol was modified to replace Tris buffers with TEAB to avoid the addition of free amine groups that interfere with iTRAQ labeling. Collected peptides were dried by vacuum evaporation and resuspended in 23.2 μL 0.5 M TEAB. An aliquot of 3.2 μL was collected from each sample and combined to create a pooled internal reference standard.

Digested peptides were labeled with 8-plex iTRAQ isobaric reagents. Benign, normal adjacent and infiltrating ductal carcinoma samples were labeled with the 113−119 m/z iTRAQ reagents. Thirteen equal aliquots of 20 μL of the pooled control were labeled with the 121 m/z iTRAQ reagent. Individually labeled pooled reference standards were combined into one tube, vortexed and spun briefly to mix and then separated into single-use tubes. After labeling, each 8-plex sample set was combined and one aliquot from each set was diluted to 2 mL using 0.1% trifluoroacetic acid (TFA) and desalted on an ENVI-18 3 mL solid phase extraction (SPE) cartridge (Supelco). Eluates from SPE were evaporated to near dryness on a speed-vacuum centrifuge and resuspended in strong cation exchange buffer A for chromatographic separation.

Peptide Analysis

Chromatographic fractionation was performed through a 2.1 × 200 mm Polysulfethyl strong cation exchange (SCX) column (PolyLC). Positively charged tryptic peptides were eluted through a linear gradient of KCl from 0 to 0.09 M in 15 min, and 0.09 to 0.36 M in 7 min. Fractions were collected every minute into a 96-well plate. Eluted peptides were pooled into 12 fractions per set, desalted using C18 StageTips[14] and speed-vacuumed to dryness.

Chromatographic spotting was performed on an Agilent 1100 series LC system on a house-packed nanocolumn using 3.5 μm C18 particles (Symmetry C18, Waters) in a 75 μm x 150 mm fused silica capillary. Each fraction was resuspended in 8 μL of 0.1% TFA and loaded onto a Zorbac C18 (0.3 × 5 mm, Agilent) trap column. Peptides were eluted by linear gradient of acetonitrile from 0 to 35% in 120 min. A nanomixing tee combined elutions with (Matrix-assisted laser desorption/ionization) MALDI matrix delivered at 1.2 μL/min. The matrix consisted of 5.0 mg/mL recrystallized α-Cyano-hydroxycinnamic acid (CHCA) (Sigma) prepared in 70% acetonitrile (ACN), 0.1% TFA, 10 mM ammonium phosphate monobasic spiked with 2.5 fmol/μL ACTH 18−39 as an internal standard. Fractions were spotted every 10 s on a blank LC−MALDI plate (ABSciex). Calibration mix containing 6-peptide standards (ABSciex) was manually spotted on all calibration spots prior to LC-spotting.

Spotted plates were analyzed with a 4800 MALDI time-of-flight (TOF/TOF) analyzer (ABSciex). The 4800 6-peptide Cal Mix (ABI) was spotted on all calibration spots for external calibration for both reflector MS and MS/MS mode. MS data was collected in reflector positive mode with 1000 laser shots and processed with internal calibration to ACTH (18−39). MS/MS data was collected in 2 keV mode with up to 2000 laser shots collected per spectrum. The top 10 precursors on each spot were fragmented starting from the weakest, followed by

dx.doi.org/10.1021/pr201018y | J. Proteome Res. 2012, 11, 2236−2246

fragmentation of the next 10 precursors starting from the strongest. The two sets of data were combined for analysis.

Data Analysis

Data sets were imported to ProteinPilot (ABI, version 4.0.8085) for identification of peptides from tandem mass spectra using the Paragon Algorithm[9] and protein inference via the Pro Group Algorithm. Briefly, the Paragon Algorithm evaluates each observed mass spectra against theoretical peptide spectra to calculate a confidence metric on the basis of matches to multiple de novo sequence tags and the frequency of various modifications, substitutions and digestion events. Observed spectra were mapped against the Uniprot-sprot database (version 57.2, updated May, 2009) in thorough ID mode under the following parameters: *H. sapiens* as species, Cys Alkylation by iodoacetamide, iTRAQ labeling at K residues and n-termini, and trypsin digestion. In addition to the Paragon confidence metric, global and local false discovery rates were estimated by searching a concatenated target-decoy database, in which decoys were derived by reversing sequences in the protein database. Identified peptides were analyzed to infer detected proteins through the use of the Pro Group Algorithm. This process is impaired by the "one to many" relationship of spectra to peptides and peptides to proteins. The ambiguity in assigning spectra to detected proteins is alleviated by reporting the minimal set of proteins justified by the spectral evidence. Detected proteins were ranked on the basis of the unused ProtScore, a measure of the spectral evidence for a protein that is not redundant with a higher ranking protein. Protein groups with an unused ProtScore greater than or equal to 1.3 (95% confidence) were defined as detected. Within each protein group, the protein with the most spectral evidence supporting it was selected for downstream quantitative analysis. If more than one protein was supported with equal spectral evidence in a given protein group, both proteins were included as there is no evidence to support the presence of one protein over the other.

Raw areas and associated errors of reporter ion peak measurements as determined by Protein Pilot were exported to the R Statistical Environment[15] for normalization, summarization, and missing value imputation. Reporter ion peak areas were adjusted to account for isotopic overlap using the default correction factors. Prior to normalization, signals associated with questionable spectra (i.e., no iTRAQ modification, low signal-to-noise, duplicate hits, missing data in the pooled reference standard channel) were removed. Reporter ion peak areas were converted into log base 2 expression ratios of experimental iTRAQ channels over the pooled standard and normalization functions were defined to adjust the median expression ratio of each sample to zero and standardize the variance across samples using loess regression and global scale normalization. At this stage, any signals that were not included for protein quantification (i.e., contaminants, decoy hits, low-confidence peptides) were removed. Normalization functions were applied to remove technical bias both within and across iTRAQ sets and data from each iTRAQ set was merged into one data set using the Uniprot Identifier of the associated protein to assign peptide-level data in each set of iTRAQ labeled samples to the appropriate protein groups. Protein scale log-ratios, X_j, were calculated using a weighted average of peptide scale measurements, x_i, as follows:

$$X_j = \frac{\sum_{i=1}^{N} w_i x_i}{\sum_{i=1}^{N} w_i} \quad (1)$$

$$w_i = 1/\sqrt{\left(\frac{\text{Error A}}{\text{Area A}}\right)^2 + \left(\frac{\text{Error B}}{\text{Area B}}\right)^2} \times 100 \quad (2)$$

in which the weight, w_i, is the percent error of the two peak areas in the *ith* log-ratio. Following protein summarization, missing values were imputed using a K-nearest neighbor algorithm ($K = 5$).[16] To maximize the accuracy of the missing value algorithm, only proteins with less than or equal to 50% missing data were imputed. Missing values in other proteins were marked as NA.

Significantly differentially expressed proteins were identified using a two-sample *t* test to compare the log-ratios of reporter ion peak areas in each pair wise comparison of benign vs IDC, benign vs normal and normal vs IDC. The false discovery rate was calculated using the method of Benjamini and Hochberg to control for multiple testing.[17]

The gene set enrichment analysis (GSEA) methodology[18] was used to identify sets of functionally related proteins that are differentially expressed in each of the three pairwise comparisons of benign vs IDC, benign vs normal and normal vs IDC. Prior to GSEA, data associated with protein isoforms were removed. This step is necessary with the use of gene-centric pathway databases as functional mapping from genes to protein isoforms is not guaranteed. In some instances proteins were observed in different protein groups across the different iTRAQ labeled sets of samples. When this occurred, this resulted in the association of these proteins with multiple expression values. In order to generate a unique expression value for each protein, we summarized the expression value of these proteins to the median value for each sample. This solution is commonly used in a similar situation in gene expression microarray analysis when multiple probes are targeted to the same gene. Gene set enrichment analysis was implemented using the GSEA Preranked tool in the java-based GSEA application. In each comparison, proteins were ranked according to the t-statistic from the two-sample *t* test. Gene sets were obtained from the curated gene set collection of the Molecular Signatures database. Specifically, gene sets of canonical signaling pathways from the Kyoto Encyclopedia of Genes and Genomes (KEGG), Reactome and Biocarta databases were compiled. Prior to enrichment analysis, Entrez Gene identifiers in each gene set were translated into Uniprot identifiers for compatibility with protein data. A false discovery rate of 0.25 was used to identify significantly deregulated pathways, as described.[18]

Significantly deregulated pathways identified by GSEA were visualized and organized using the Enrichment Map plug-in[19] for Cytoscape.[20] A network was generated in which nodes represent pathways and edges link pathways with common proteins. The overlap between proteins was calculated using the Jaccard coefficient,[19] with the default threshold of 0.25.

RESULTS

Identification of Differentially Expressed Proteins

Protein expression profiles of 90 frozen tissue samples of IDC, benign breast growths or normal adjacent tissue were analyzed

dx.doi.org/10.1021/pr201018y | J. Proteome Res. 2012, 11, 2236−2246

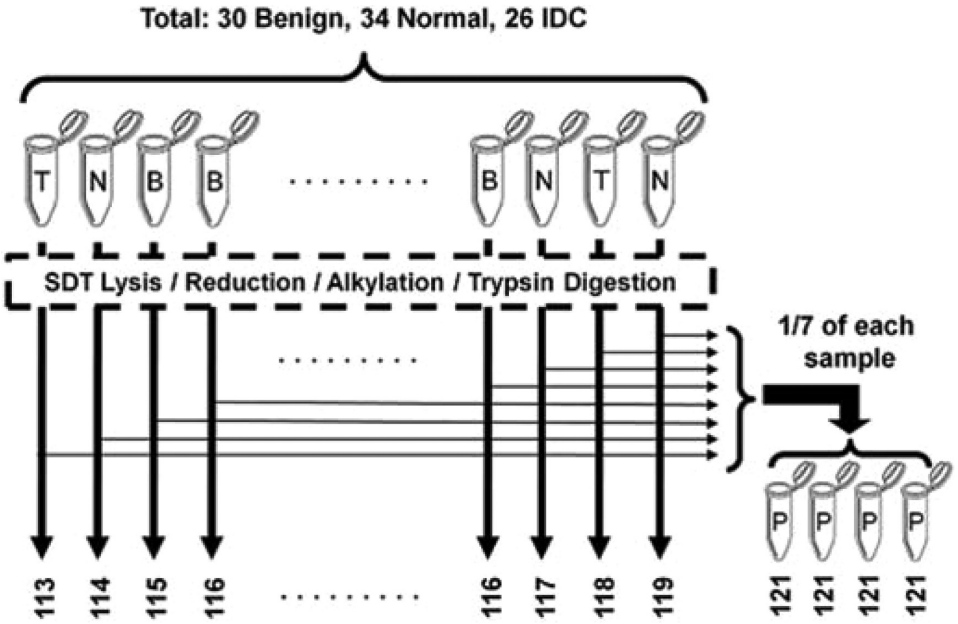

Figure 1. Diagram of experimental design. T represents tumor, N normal, B benign, P pooled reference standard.

using label-based quantitative 2D LC−MS/MS. Figure 1 illustrates the experimental design. To analyze 90 samples, 13 sets of iTRAQ 8-plex isobaric tags were required. The distribution of the samples into the iTRAQ sets is given in Supporting Information Table 1. The 121 m/z isobaric tag was used to label an aliquot of the pooled standard in each of the 13 iTRAQ experiments. Positive identifications were determined at the 95% confidence level. Global false discovery rates between 0.003 and 0.02 were observed at the 95% confidence level (Supporting Information Table 2). A total of 6023 peptides (Supporting Information Table 3) and 853 proteins (Supporting Information Table 4) were identified across all experiments.

Proteins that exhibit statistically significant differential expression patterns in the progression of breast cancer were identified by three pairwise comparisons of expression in IDC, benign and normal samples (Supporting Table 5). Expression of differentially expressed proteins is depicted in a heatmap shown in Figure 2A in which columns represent samples and rows represent proteins. Red/green regions of the heatmap indicate up-regulation/down-regulation in the sample relative to the pooled reference standard. Samples and proteins with similar expression patterns are grouped using the Pearson correlation metric and average linkage hierarchical clustering. The sample color bar indicates benign (blue), normal adjacent (green) and IDC (red) samples. Samples cluster into three groups that correlate well with the known sample classifications (Figure 2B). Two-hundred seventy-five proteins with differential expression patterns in at least one of the three pairwise comparisons were identified (Figure 2A). An equal number of 193 differentially expressed proteins were detected in the comparisons of benign vs IDC tissue and normal vs IDC tissue. A smaller number of 72 proteins were differentially expressed in benign breast growths vs normal adjacent tissue.

Inference of Differentially Expressed Pathways

Significantly deregulated signaling pathways were identified using a set enrichment analysis approach.[18] Sets of functionally related proteins that interact in canonical signaling pathways such as the MAPK pathway were identified using information from the Molecular Signatures database.[18] Each of the three pairwise comparisons of tumor, benign and normal samples were considered separately. Proteins were ordered from the most up-regulated to most down-regulated according to the value of the t-statistic. Deregulated pathways were identified using a Kolmogorov-Smirnoff like statistic calculated by tabulating a weighted sum each time a pathway protein was encountered while traveling the order list from most up-regulated to most down-regulated. We report a number of cancer-related pathways that are deregulated in both benign breast growths and normal adjacent tissue vs IDC (Tables 1 and 2). Thirty-two pathways were significantly up-regulated and seven pathways were significantly down-regulated in IDC.

To facilitate interpretation of set enrichment analysis, we generated an enrichment map that links deregulated pathways that share a significant fraction of common proteins. In this manner, we associated sets of deregulated pathways with biological functions relevant to cancer progression. Figure 3 shows this network of deregulated cancer mechanisms in which nodes represent pathways that are deregulated in IDC vs benign breast growths (node center) or normal tissue (node border). Nodes are colored according to the significance of enrichment and the size of each node is related to the number of proteins in the associated pathway. An edge between nodes A and B indicates that a significant number of proteins in pathways A and B are common to both pathways. The thickness of the edge indicates the fraction of the common proteins relative to the total number of proteins in each pathway. Pathways associated with common biological functions were manually clustered and labeled. The enrichment map visualization indicates the up-regulation of pathways related to transcript and protein metabolism and molecular pathways implicated in regulation of oncogenic mechanisms. In contrast, proteins related to lipid metabolism were down-regulated in IDC. A number of deregulated pathways related to the immune response and metastasis were also identified.

dx.doi.org/10.1021/pr201018y | J. Proteome Res. 2012, 11, 2236−2246

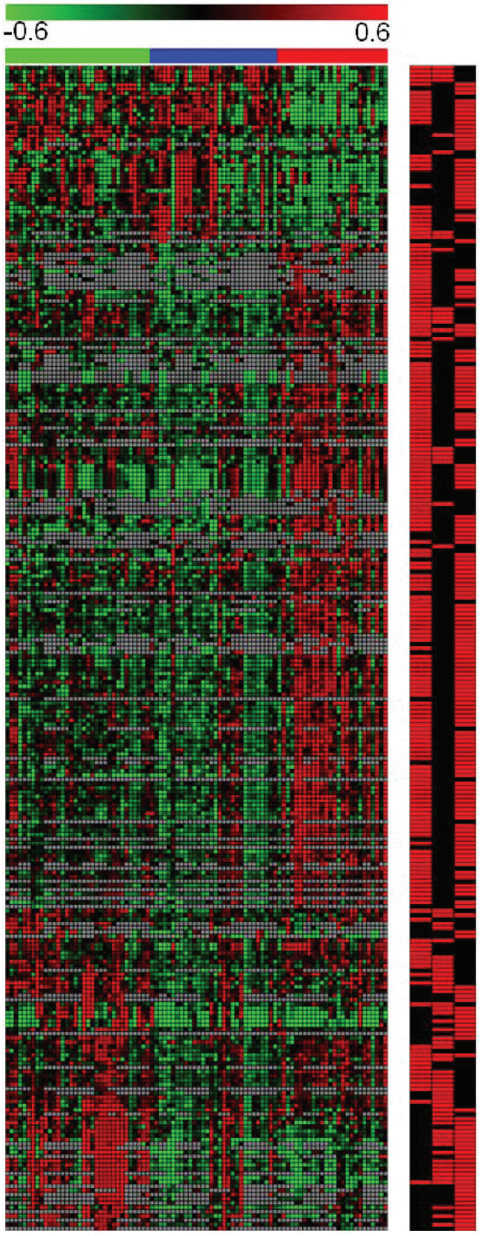

Figure 2. Heatmap of proteins differentially expressed in the comparison of IDC, normal and benign tissue. Proteins (rows) clustered by Pearson correlation and average linkage. Samples (rows) ordered according to tissue classification. Green represents down-regulation, red represents up-regulation, gray represents missing value. Sample color bar indicates benign (blue), normal (green) and IDC (red) tissue samples. Red bars in protein color bar indicates significant deregulation in the comparison of benign vs IDC, benign vs normal and normal vs IDC from left to right.

Up-regulation of Canonical Oncogenes

Comparison of protein expression in IDC in contrast to benign breast growths or normal breast tissue resulted in the identification of 263 proteins that are deregulated in breast cancer progression. A number of proteins implicated in the regulation of cancer-related mechanisms and annotated in a compilation of cancer-related pathways in the KEGG database were significantly up-regulated in IDC vs benign tissue. This signature was driven by the up-regulation of oncogenic proteins like CTNBB1, STAT1, FGFR1, GLUT1, and RAL GTPases. Previous studies have identified associations between up-regulation or constitutive activation of these proteins and breast cancer onset and progression.[21−25] Detection of the deregulation of these canonical oncogenic proteins supports the use of our methodology.

Deregulation of Metabolism of Macromolecules

Enrichment map analysis indicated up-regulation of 21 pathways related to the metabolism of proteins and transcripts in IDC relative to benign or normal tissue. Up-regulation of pathways related to translation is mediated by the up-regulation of ribosomal subunits, and translation initiation and translation elongation factors which catalyze protein synthesis. Up-regulation of transcription related pathways is inferred by the relatively high expression of histone proteins, polymerase I transcript release factor and components of the spliceosome. Similarly, the mRNA processing signature is composed of proteins including nuclear riboproteins, splicing factors, and heat shock proteins.

In contrast, proteins related to lipid and lipoprotein metabolism were down-regulated in IDC. This signature likely reflects alterations in lipid metabolism due to the increased demand for energy production in the tumor. Many of the down-regulated proteins in the lipid metabolism signature, such as apolipoproteins and hormone-sensitive lipase, are related to lipid transport and hydrolysis.[26,27] Tumors and other highly proliferative cells generate lipid precursors de novo, from intermediates produced during aerobic glycolysis.[28] Proteins related to de novo metabolism of fatty acids, such as HADHA, HADHB and ECHS1, are up-regulated in tumor relative to benign tissue.

Deregulation of Immune Response Pathways

Enrichment set analysis detected the deregulation of four molecular signaling pathways related to the immune response. Three pathways, including antigen-processing and presentation, endocytosis and a general immune signaling pathway, were up-regulated in IDC. Up-regulation of these pathways is driven by the increased expression of proteins related to the adaptive immune response, such as MHC proteins,[29,30] TAP1,[29,30] and SLC3A2.[31] Conversely, proteins related to the innate immune response through complement and coagulation cascades were down-regulated in tumor samples. These pathways enhance the immune response through proteolytic cascades that result in the activation of cell death pathways in foreign cells and recruitment of inflammatory and immunocompetent cells.[32] The main effectors of the complement cascade (C1Q, C4, C3)[33] are down-regulated in tumor samples relative to benign and normal conditions.

Deregulation of Pathways Related to Invasion and Metastasis

Seven pathways related to the regulation of invasion and metastasis were deregulated in IDC relative to benign and normal conditions. A number of pathways including integrin cell surface interactions, extracellular matrix interactions, focal adhesion, NCAM signaling and PDGF signaling were down-regulated in IDC. These pathways interact with extracellular matrix components to initiate signaling cascades that regulate processes such as cell motility, proliferation and survival. Down-regulation of these pathways was mediated by decreased expression of extracellular matrix (ECM) proteins including collagens, laminins, vitronectin and tenascin. Notably, intracellular elements of the focal adhesion pathway and proteins

dx.doi.org/10.1021/pr201018y | J. Proteome Res. 2012, 11, 2236−2246

Table 1. Molecular Signaling Pathways that are Up-regulated in IDC vs Benign or Normal Tissue

			benign vs tumor			normal vs tumor		
	database	pathway name	size[a]	NES[b]	FDR[c]	size[a]	NES[b]	FDR[c]
translation	Reactome	formation of a pool of free 40S subunits	73	−1.89	1.44×10^{-4}	73	−2.38	0
	KEGG	ribosome	69	−1.92	0	69	−2.4	0
	Reactome	formation of the ternary complex and subsequently the 43S complex	32	−1.93	0	32	−2.24	0
	Reactome	gene expression	114	−1.77	9.54×10^{-4}	115	−2.47	0
	Reactome	translation	78	−1.88	1.33×10^{-4}	78	−2.41	0
	Reactome	translation initiation complex formation	33	−1.91	0	33	−2.27	0
	Reactome	GTP hydrolysis and joining of the 60S ribosomal subunit	74	−1.92	0	74	−2.46	0
	Reactome	metabolism of proteins	95	−1.84	1.15×10^{-4}	95	−2.35	0
	Reactome	peptide chain elongation	72	−1.95	0	72	−2.42	0
transcription	Reactome	RNA polymerase I III and mitochondrial transcription	23	−1.62	0.007	23	−1.52	0.043
	Reactome	RNA polymerase I promoter clearance	21	−1.67	0.004	21	−1.83	0.002
	Reactome	RNA polymerase I promoter opening	21	−1.68	0.004	21	−1.84	0.002
	Reactome	packaging of telomere ends	19	−1.63	0.006	19	−1.76	0.005
	Reactome	telomere maintenance	19	−1.65	0.005	19	−1.74	0.006
	Reactome	transcription	33	−1.53	0.023	33	−1.6	0.024
mRNA processing	Reactome	elongation and processing of capped transcripts	34	−1.39	0.085	35	−1.87	0.002
	KEGG	spliceosome	33	−1.3	0.15	33	−1.57	0.031
	Reactome	processing of capped intron containing pre mRNA	33	−1.36	0.107	34	−1.83	0.002
	Reactome	mRNA splicing	33	−1.39	0.087	34	−1.82	0.002
	Reactome	formation and maturation of mRNA transcript	34	−1.4	0.084	35	−1.86	0.002
immune response	KEGG	antigen processing and presentation	18	−1.85	1.24×10^{-4}	18	−2.07	6.25×10^{-5}
	KEGG	endocytosis	16	−1.36	0.106			
	Reactome	signaling in immune system				29	−1.3	0.191
cell motility	Reactome	semaphorin interactions	16	−1.48	0.041			
	KEGG	regulation of actin cytoskeleton	27	−1.44	0.058			
	KEGG	pathways in cancer	17	−1.42	0.069			

[a]Number of proteins in the pathway after filtering out proteins not measured in the data set. [b]Normalized Enrichment Score − running sum statistic that indicates functional enrichment, normalized according to the size of the protein set. [c]False Discovery Rate − probability that enrichment represents a false positive finding, calculated by permuting protein IDs in the data set.

Table 2. Molecular Signaling Pathways that are Down-regulated in IDC vs Benign or Normal Tissue

			benign vs tumor			normal vs tumor		
	database	pathway name	size[a]	NES[b]	FDR[c]	size[a]	NES[b]	FDR[c]
cell motility	KEGG	ECM receptor interaction	26	2.66	0	26	1.62	0.053
	KEGG	focal adhesion	40	1.68	0.018	40	1.74	0.031
	Reactome	integrin cell surface interactions	20	1.92	0.008	20	1.26	0.228
	Reactome	NCAM signaling for neurite out growth	18	2.36	7.04×10^{-4}	18	1.31	0.212
	Reactome	signaling by PDGF	16	2.24	5.63×10^{-4}			
immune response	KEGG	complement and coagulation cascades	22	2.72	0	22	1.74	0.038
	Reactome	metabolism of lipids and lipoproteins	26	2.49	9.39×10^{-4}	26	2.41	0

[a]Number of proteins in the pathway after filtering out proteins not measured in the data set. [b]Normalized Enrichment Score − running sum statistic that indicates functional enrichment, normalized according to the size of the protein set. [c]False Discovery Rate − probability that enrichment represents a false positive finding, calculated by permuting protein IDs in the data set.

related to regulation of the actin cytoskeleton such as filamin, actinin, vinculin, myosin, actin and effectors of RhoGTPases are up-regulated in IDC relative to benign breast growths.

DISCUSSION

Breast cancer is a complex disease characterized by the deregulation of molecular signaling pathways that leads to the acquisition of oncogenic phenotypes. Molecular profiling provides the means to systematically identify deregulated pathways in breast cancer progression. In this study, we developed methods to measure protein expression in large numbers of samples based on quantitative label-based mass spectrometry. These methods were applied to identify proteins and associated signaling pathways that are deregulated in the comparison of infiltrating ductal carcinoma to benign breast growths or normal mammary tissue.

Experimental design is an important consideration in expression profiling studies to enable the estimation and removal of technical variation. In label-based quantitative proteomics, technical variation arises from small differences in sample handling and preparation, labeling efficiency, and run-specific effects of liquid chromatography and mass spectrometry. To correct for these effects, we incorporated an internal reference standard, consisting of an equal amount of protein from each tissue sample, into each iTRAQ set. This design can be viewed as an extension of the reference design commonly

dx.doi.org/10.1021/pr201018y | J. Proteome Res. 2012, 11, 2236−2246

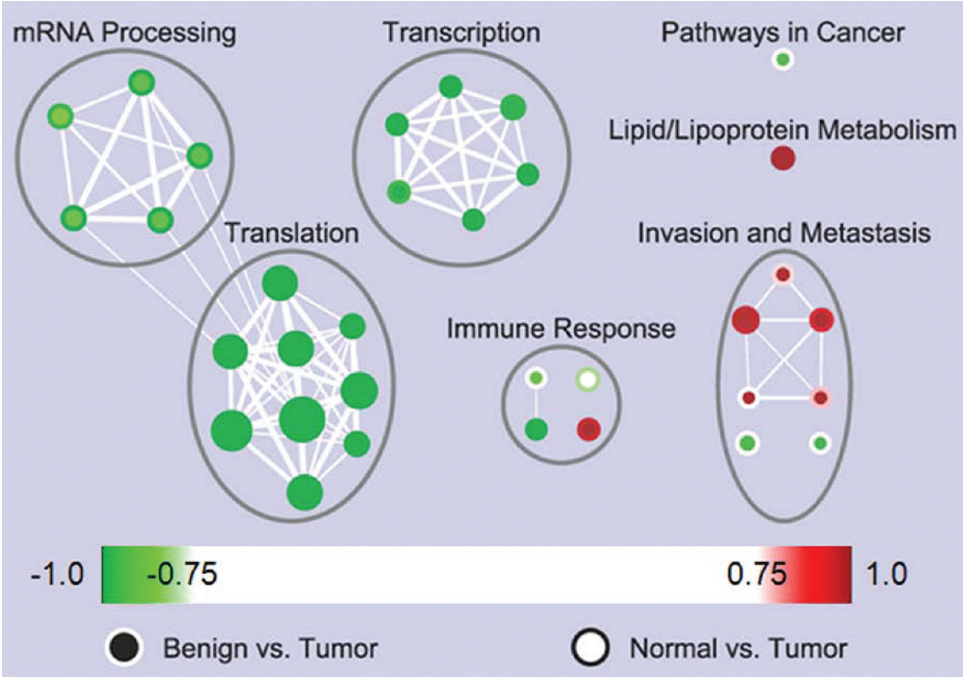

Figure 3. Enrichment map visualization of significantly deregulated molecular signaling pathways. Nodes represent deregulated pathways. Nodes colored according to the significance of enrichment (i.e., false discovery rate). Green indicates down-regulation and red indicates up-regulation of pathways in benign or normal tissue relative to IDC. Node center, Benign vs IDC; Node border, Normal vs IDC. Node size associated with number of proteins detected in pathway. Edges indicate the fraction of shared proteins between pathways. Nodes were manually clustered and labeled to identify deregulated cellular mechanisms.

used in two-color microarray or differential gel electrophoresis experiments.[34] Expression values for a given sample were derived from the ratio of the associated reporter ion signal divided by reporter ion signal associated with the internal standard. Normalization of expression values relative to a common reference standard enables the removal of sample-specific and iTRAQ-set specific technical variation. The reference experimental design adopted in this study permitted the analysis of a large cohort of breast cancer tissue samples to increase the statistical power for the detection of deregulated proteins and pathways.

In tumor progression, deregulation of metabolism provides an increased supply of energy and molecules needed to support uncontrolled cellular proliferation. In support of this hypothesis, we observed the up-regulation of processes related to transcription, mRNA postprocessing and translation in IDC. In contrast, pathways related to the metabolism of lipids and lipoproteins are down-regulated. This result is counterintuitive as fatty acids are required for energy and the generation of structural components in rapidly dividing cells. Closer examination of deregulated proteins related to lipid metabolism suggests that this signature may instead be indicative of altered metabolic processes in the tumor microenvironment. Cells acquire resources to support lipid metabolism through either digestion and mobilization of dietary lipids or de novo synthesis from metabolic precursors. A majority of the proteins related to lipid metabolism that are down-regulated in IDC are involved in the transport of lipids or hydrolysis of lipids in adipose tissue. These observations indicate a shift away from the metabolism of dietary lipids and toward de novo synthesis in the tumor microenvironment of IDC. This phenomenon is a common hallmark of oncogenic transformation across tumor types.[35] In addition, alterations of lipid metabolism mechanisms are a general consequence of the Warburg effect in which cells in tumor tissue shift to energy production based on aerobic glycolysis.[28] In highly proliferative cells, lipid synthesis can be driven by production of acetyl-CoA from intermediate metabolites of the TCA cycle. We have detected the up-regulation of proteins involved in beta-oxidation, a similar mechanism by which cells can produce acetyl-CoA. Taken together, these results suggest that the observed down-regulation of lipid metabolism pathways may point to mechanisms by which metabolic pathways are altered in cancer cells to promote proliferation in the tumor microenvironment.

In addition to its roles in energy production and lipid biosynthesis, acetyl-CoA is a substrate that provides acetyl groups for lysine acetylation of signaling proteins and histones. This suggests that the up-regulation of beta oxidation in IDC may improve tumor fitness through the deregulation of cellular signaling pathways and epigenetic modification. Histone acetylation induces chromatin remodeling to facilitate gene transcription. Increased levels of histone acetylation have been associated with tumor progression. Global hyperacetylation of histones has been associated with high grade and tumor recurrence in prostate cancer.[36] Similar levels of hyper-acetylation have been observed in other cancers including hepatocellular carcinoma.[37] In addition, a number of oncogenic and tumor suppressor signaling cascades are regulated by acetylation.[38] Increased production of acetyl-CoA through deregulation of beta-oxidation along with altered function of acetyltransferases and deacetylases may provide the resources needed for epigenetic modification and deregulation of cellular signaling pathways that promote tumorigenesis.

One of the mechanisms by which cancer cells can escape the immune response is by the inhibition of antigen processing and presentation pathways that catabolize intra- and extracellular

dx.doi.org/10.1021/pr201018y | J. Proteome Res. 2012, 11, 2236–2246

proteins and present them to immune effector cells. Specifically, down-regulation of major histocompatibility proteins, TAP1 and other components of the immunoproteasome or loss of sensitivity to interferon signaling through the JAK-STAT1 pathway can inhibit antigen presentation and subsequent T cell activation.[39,40] Notably, in this study we detected up-regulation of the antigen processing and presentation machinery and the STAT1 protein in IDC tissue. This finding may suggest that the immune response induced by presentation of IDC antigens is insufficient to eliminate the tumor. Alternatively, it has been demonstrated that antigen presentation by immature immune cells can induce tolerance through deletion or deactivation of T cells,[41] or generation of immunosuppressive regulatory T cells.[42] Tumor driven mechanisms to inhibit the maturation of antigen presenting cells have been observed.[43] Finally, alternative mechanisms of immune evasion may be operating in IDC. For example, secretion of immunosuppressive cytokines, such as TGF-beta, FASLG, or IDO can inhibit T cell and natural killer cell function or drive the transformation of effector T cells into regulatory T cells.[44] These mechanisms would circumvent proper activation of antigen presentation cells to suppress the immune response. Further investigation is needed to validate the observed up regulation of the antigen presentation pathways in IDC tissue and determine whether this up-regulation contributes to immune tolerance in breast cancer.

In contrast to the up-regulation of proteins involved in adaptive immunity, proteins that mediate the complement and coagulation cascades, a component of the innate immune system, were down-regulated in IDC. The complement cascade has been associated with both pro- and antitumorigenic functions. Complement effectors support immune function by mediating direct attack on foreign cells through the membrane attack complex[45] or recruiting and activating immune effector cells.[32] As such, down-regulation of proteins involved in the complement system may contribute to immune escape. In contrast, the complement system is also a potent activator of inflammation.[33] A pro-inflammatory microenvironment enhances tumor progression through genetic instability as a result of DNA damage, increased proliferation, remodeling of the extracellular matrix required for invasion and metastasis, and activation of angiogenesis.[46] Given the opposing effects of complement on tumorigenesis, it is reasonable to assume that different tumor types may have developed different mechanisms to contend with it. Tumors which down-regulate complement can benefit from a decrease in immunosurveillance and may induce other mechanisms to promote oncogenic phenotypes in the absence of inflammation. Alternatively, tumors which induce up-regulation of complement would receive the benefits of an inflammatory microenvironment and may adopt other methods of interfering with the immune response. Our results suggest that IDC generally falls under the former description. This observation has therapeutic implications as tumors exhibiting deactivation of complement may benefit from immunotherapy designed to counteract the negative impact on immune function.

Metastasis is implemented by a multistep process involving invasion of the local tissue, intravasation into, transit, and extravasation from the circulation and lymphatic system, and formation of tumors at distant sites. In this study, we observed evidence of a pro-migratory phenotype through the activation of pathways related to remodeling of the actin cytoskeleton. RhoGTPases regulate actin cytoskeleton dynamics and promote cell motility. In animal models, inhibition of RhoGTPase activation results in reduced intravasation and lung metastases.[47] Identification of RhoA expression as a marker of progression in primary breast cancer cells suggests the relevance of this mechanism in IDC.[48] We detected up-regulation of ARHGEF12, a rho guanine nucleotide exchange factor that activates RhoGTPases. We also observed the up-regulation of various actin and myosin proteins subunits. Increased expression of actin and myosin may enable the formation of actin filaments and stress fibers that enable cell movement.[49] Cell motility is also facilitated by turnover of focal adhesion complexes.[49] Formation of focal adhesions at the leading edge of the cell permits anchoring of the cell to the extracellular matrix. Similarly, disassembly of focal adhesions at the terminal edge allows cells to move in the direction of migration. We observed up-regulation of a number of focal adhesion proteins, including actinin, filamin, talin and vinculin, in IDC. Up-regulation of focal adhesion proteins may enable the increased turnover of focal adhesions observed in migrating cells.

In addition to intracellular modifications that promote cell motility, metastasis is promoted by cross-talk between cancer cells and the tumor-associated stroma.[50] Progression of normal mammary tissue to IDC is characterized by malfunction and loss of myoepithelial cells that produce components of the basement membrane. Investigation of gene expression in DCIS- and tumor-associated myoepithelial cells demonstrates deficiencies in the production of laminin.[51,52] Similarly, expression of collagen is reduced in stage II and III breast cancer.[53] In vitro studies indicate that breast cancer cells signal for the down-regulation of collagen production in tumor-associated fibroblasts. Decreased collagen production was observed in normal fibroblasts cocultured with MCF7, MDA-MB-231, T47D, and ZR-75−1 breast cancer cells.[53] A similar effect was observed in fibroblasts grown in tumor conditioned medium, suggesting that down-regulation of collagen production is induced by paracrine signaling from breast cancer cells.[53] In this study, we observed the down-regulation of five pathways related to invasion and metastasis. Down-regulation of laminins, collagens and other basement membrane proteins was a common component in all of these pathways. This molecular signature may be an indicator of reduced extracellular matrix production signaled by IDC cells and mediated by the tumor-associated stroma to allow for tissue remodeling and promote local invasion.

■ CONCLUSIONS

Breast cancer is characterized by the deregulation of a range of cellular processes and molecular signaling pathways that promote tumorigenesis. In this study, we developed a methodology for the identification and quantification of proteins in large numbers of frozen tissue samples using label-based 2D-LC−MS/MS. Using this methodology, we measured protein expression in ninety frozen tissue samples classified by histology as IDC, benign breast growths or normal adjacent tissue. In total, we identified 853 proteins, 265 of which exhibit differential expression patterns in IDC relative to either benign breast growths or normal adjacent tissue. Using functional set enrichment analysis, we identified 32 canonical signaling pathways that are deregulated in benign or normal adjacent tissue relative to IDC. Examination of these pathways revealed the deregulation of a number of mechanisms related to cancer progression including invasion and metastasis and the

immune response. Deregulation of these pathways points to the complex relationship between tumor cells and the surrounding microenvironment. Further experimental and clinical investigation of these deregulated pathways and the associated proteins may lead to more accurate diagnoses and may provide new druggable targets for targeted cancer therapy.

■ ASSOCIATED CONTENT

Supporting Information

Supporting Table 1. Sample annotation. Each sample is described using a unique specimen accession number. Sample information includes a number indicating which set of 8-plex iTRAQ reagents was used for labeling as well as the m/z of the iTRAQ reporter ion peak and a class label to indicate the histology based classification of the associated tissue. Supporting Table 2. Global and local false discovery rate associated with the 95% confidence level for protein identification for each independently analyzed set of iTRAQ labeled samples. False discovery rates are calculated using the target decoy strategy as described in the methods section and the Supporting Information. Global false discovery rate indicates the proportion of proteins that are likely to be falsely identified. Local false discovery rate indicates the probability that a protein with a 95% confidence in identification is likely to be falsely identified. Supporting Table 3. Peptide specific information used for identification of spectra and quantification of the abundance of the associated peptides and proteins. All information was obtained from ProteinPilot (ABI, version 4.0.8085). Each worksheet in the Excel file is associated with a different set of independently analyzed iTRAQ labeled samples as indicated by the worksheet label. Each row represents an independent spectral measurement. See Supporting Information for more details. Supporting Table 4. Protein specific information used for the identification. All information was obtained from ProteinPilot (ABI, version 4.0.8085). Each worksheet in the Excel file is associated with a different set of independently analyzed iTRAQ labeled samples as indicated by the worksheet label. Each row represents a uniquely identified protein. See Supporting Information for more details. Supporting Table 5. Linked Protein and Peptide specific information is presented to facilitate interpretation. See the description of Supporting Table 3 and Supporting Table 4 in Supporting Information for a detailed description of the data in each column. Supporting Table 6. Proteins that are differentially expressed in at least one of the three pairwise comparisons of infiltrating ductal carcinoma, benign breast growths and normal adjacent tissue. Proteins are annotated with Uniprot Identifiers as well as EntrezGene identifiers, gene symbols and gene names when possible. Summary statistics including the mean and standard deviation of expression in each tissue class is listed. Logical indicators describe which proteins are differentially expressed in which comparison. This material is available free of charge via the Internet at http://pubs.acs.org.

■ AUTHOR INFORMATION

Corresponding Author

*Telephone: 215-503-9273. Fax: 215-503-9274. E-mail: Andrew.Quong@jefferson.edu.

Notes

The authors declare no competing financial interest.

■ ACKNOWLEDGMENTS

This work was supported by a grant from the Breast Cancer Research Foundation. Tissues were obtained through the tumor bank at the Kimmel Cancer Center at Thomas Jefferson University supported by the Cancer Center support grants from the NCI.

■ LIST OF ABBREVIATIONS

2D-LC−MS/MS, two-dimensional liquid chromatography−tandem mass spectrometry; IDC, infiltrating ductal carcinoma; SDS, sodium dodecyl sulfate; DTT, dithiothreitol; BCA, bicinchoninic acid; FASP, filter-aided sample preparation; TEAB, triethyl ammonium bicarbonate; TFA, trifluoroacetic acid; SPE, solid phase extraction; SCX, strong cation exchange; MALDI, Matrix-assisted laser desorption/ionization; CHCA, α-cyano-4-hydroxycinnamic acid; ACN, acetonitrile; ACTH, adenocorticotrophic hormone; TOF, time-of-flight; GSEA, gene set enrichment analysis; KEGG, Kyoto Encyclopedia of Genes and Genomes; ECM, extracellular matrix

■ REFERENCES

(1) Khwaja, A.; Rodriguez-Viciana, P.; Wennstrom, S.; Warne, P. H.; Downward, J. Matrix adhesion and Ras transformation both activate a phosphoinositide 3-OH kinase and protein kinase B/Akt cellular survival pathway. *EMBO J.* **1997**, *16* (10), 2783−93.

(2) Pruitt, K.; Der, C. J. Ras and Rho regulation of the cell cycle and oncogenesis. *Cancer Lett.* **2001**, *171* (1), 1−10.

(3) Sjoblom, T.; Jones, S.; Wood, L. D.; Parsons, D. W.; Lin, J.; Barber, T. D.; Mandelker, D.; Leary, R. J.; Ptak, J.; Silliman, N.; Szabo, S.; Buckhaults, P.; Farrell, C.; Meeh, P.; Markowitz, S. D.; Willis, J.; Dawson, D.; Willson, J. K.; Gazdar, A. F.; Hartigan, J.; Wu, L.; Liu, C.; Parmigiani, G.; Park, B. H.; Bachman, K. E.; Papadopoulos, N.; Vogelstein, B.; Kinzler, K. W.; Velculescu, V. E. The consensus coding sequences of human breast and colorectal cancers. *Science* **2006**, *314* (5797), 268−74.

(4) Greenman, C.; Stephens, P.; Smith, R.; Dalgliesh, G. L.; Hunter, C.; Bignell, G.; Davies, H.; Teague, J.; Butler, A.; Stevens, C.; Edkins, S.; O'Meara, S.; Vastrik, I.; Schmidt, E. E.; Avis, T.; Barthorpe, S.; Bhamra, G.; Buck, G.; Choudhury, B.; Clements, J.; Cole, J.; Dicks, E.; Forbes, S.; Gray, K.; Halliday, K.; Harrison, R.; Hills, K.; Hinton, J.; Jenkinson, A.; Jones, D.; Menzies, A.; Mironenko, T.; Perry, J.; Raine, K.; Richardson, D.; Shepherd, R.; Small, A.; Tofts, C.; Varian, J.; Webb, T.; West, S.; Widaa, S.; Yates, A.; Cahill, D. P.; Louis, D. N.; Goldstraw, P.; Nicholson, A. G.; Brasseur, F.; Looijenga, L.; Weber, B. L.; Chiew, Y. E.; DeFazio, A.; Greaves, M. F.; Green, A. R.; Campbell, P.; Birney, E.; Easton, D. F.; Chenevix-Trench, G.; Tan, M. H.; Khoo, S. K.; Teh, B. T.; Yuen, S. T.; Leung, S. Y.; Wooster, R.; Futreal, P. A.; Stratton, M. R. Patterns of somatic mutation in human cancer genomes. *Nature* **2007**, *446* (7132), 153−8.

(5) Stephens, P. J.; McBride, D. J.; Lin, M. L.; Varela, I.; Pleasance, E. D.; Simpson, J. T.; Stebbings, L. A.; Leroy, C.; Edkins, S.; Mudie, L. J.; Greenman, C. D.; Jia, M.; Latimer, C.; Teague, J. W.; Lau, K. W.; Burton, J.; Quail, M. A.; Swerdlow, H.; Churcher, C.; Natrajan, R.; Sieuwerts, A. M.; Martens, J. W.; Silver, D. P.; Langerod, A.; Russnes, H. E.; Foekens, J. A.; Reis-Filho, J. S.; van 't Veer, L.; Richardson, A. L.; Borresen-Dale, A. L.; Campbell, P. J.; Futreal, P. A.; Stratton, M. R. Complex landscapes of somatic rearrangement in human breast cancer genomes. *Nature* **2009**, *462* (7276), 1005−10.

(6) Perou, C. M.; Sorlie, T.; Eisen, M. B.; van de Rijn, M.; Jeffrey, S. S.; Rees, C. A.; Pollack, J. R.; Ross, D. T.; Johnsen, H.; Akslen, L. A.; Fluge, O.; Pergamenschikov, A.; Williams, C.; Zhu, S. X.; Lonning, P. E.; Borresen-Dale, A. L.; Brown, P. O.; Botstein, D. Molecular portraits of human breast tumours. *Nature* **2000**, *406* (6797), 747−52.

(7) Sorlie, T.; Perou, C. M.; Tibshirani, R.; Aas, T.; Geisler, S.; Johnsen, H.; Hastie, T.; Eisen, M. B.; van de Rijn, M.; Jeffrey, S. S.; Thorsen, T.; Quist, H.; Matese, J. C.; Brown, P. O.; Botstein, D.;

Eystein Lonning, P.; Borresen-Dale, A. L. Gene expression patterns of breast carcinomas distinguish tumor subclasses with clinical implications. *Proc. Natl. Acad. Sci. U.S.A.* **2001**, *98* (19), 10869−74.
(8) Gatza, M. L.; Lucas, J. E.; Barry, W. T.; Kim, J. W.; Wang, Q.; Crawford, M. D.; Datto, M. B.; Kelley, M.; Mathey-Prevot, B.; Potti, A.; Nevins, J. R. A pathway-based classification of human breast cancer. *Proc. Natl. Acad. Sci. U.S.A.* **2010**, *107* (15), 6994−9.
(9) Shilov, I. V.; Seymour, S. L.; Patel, A. A.; Loboda, A.; Tang, W. H.; Keating, S. P.; Hunter, C. L.; Nuwaysir, L. M.; Schaeffer, D. A. The Paragon Algorithm, a next generation search engine that uses sequence temperature values and feature probabilities to identify peptides from tandem mass spectra. *Mol. Cell. Proteomics* **2007**, *6* (9), 1638−55.
(10) Gilar, M.; Olivova, P.; Daly, A. E.; Gebler, J. C. Orthogonality of separation in two-dimensional liquid chromatography. *Anal. Chem.* **2005**, *77* (19), 6426−34.
(11) Ong, S. E.; Blagoev, B.; Kratchmarova, I.; Kristensen, D. B.; Steen, H.; Pandey, A.; Mann, M. Stable isotope labeling by amino acids in cell culture, SILAC, as a simple and accurate approach to expression proteomics. *Mol. Cell. Proteomics* **2002**, *1* (5), 376−86.
(12) Ross, P. L.; Huang, Y. N.; Marchese, J. N.; Williamson, B.; Parker, K.; Hattan, S.; Khainovski, N.; Pillai, S.; Dey, S.; Daniels, S.; Purkayastha, S.; Juhasz, P.; Martin, S.; Bartlet-Jones, M.; He, F.; Jacobson, A.; Pappin, D. J. Multiplexed protein quantitation in Saccharomyces cerevisiae using amine-reactive isobaric tagging reagents. *Mol. Cell. Proteomics* **2004**, *3* (12), 1154−69.
(13) Wisniewski, J. R.; Zougman, A.; Nagaraj, N.; Mann, M. Universal sample preparation method for proteome analysis. *Nat. Methods* **2009**, *6* (5), 359−62.
(14) Rappsilber, J.; Mann, M.; Ishihama, Y. Protocol for micro-purification, enrichment, pre-fractionation and storage of peptides for proteomics using StageTips. *Nat. Protoc.* **2007**, *2* (8), 1896−906.
(15) R Development Core Team *R: A Language and Environment for Statistical Computing*; R Foundation for Statistical Computing: Vienna, Austria, 2006.
(16) Troyanskaya, O.; Cantor, M.; Sherlock, G.; Brown, P.; Hastie, T.; Tibshirani, R.; Botstein, D.; Altman, R. B. Missing value estimation methods for DNA microarrays. *Bioinformatics* **2001**, *17* (6), 520−5.
(17) Benjamini, H.; Hochberg, Y. Controlling the false discovery rate: a practical and powerful approach to multiple testing. *J. R. Stat. Soc., Ser. B: Methodolog.* **1995**, *57* (1), 289−300.
(18) Subramanian, A.; Tamayo, P.; Mootha, V. K.; Mukherjee, S.; Ebert, B. L.; Gillette, M. A.; Paulovich, A.; Pomeroy, S. L.; Golub, T. R.; Lander, E. S.; Mesirov, J. P. Gene set enrichment analysis: a knowledge-based approach for interpreting genome-wide expression profiles. *Proc. Natl. Acad. Sci. U.S.A.* **2005**, *102* (43), 15545−50.
(19) Merico, D.; Isserlin, R.; Stueker, O.; Emili, A.; Bader, G. D. Enrichment map: a network-based method for gene-set enrichment visualization and interpretation. *PLoS One* **2010**, *5* (11), e13984.
(20) Shannon, P.; Markiel, A.; Ozier, O.; Baliga, N. S.; Wang, J. T.; Ramage, D.; Amin, N.; Schwikowski, B.; Ideker, T. Cytoscape: a software environment for integrated models of biomolecular interaction networks. *Genome Res.* **2003**, *13* (11), 2498−504.
(21) Bodemann, B. O.; White, M. A. Ral GTPases and cancer: linchpin support of the tumorigenic platform. *Nat. Rev. Cancer* **2008**, *8* (2), 133−40.
(22) Chin, K.; DeVries, S.; Fridlyand, J.; Spellman, P. T.; Roydasgupta, R.; Kuo, W. L.; Lapuk, A.; Neve, R. M.; Qian, Z.; Ryder, T.; Chen, F.; Feiler, H.; Tokuyasu, T.; Kingsley, C.; Dairkee, S.; Meng, Z.; Chew, K.; Pinkel, D.; Jain, A.; Ljung, B. M.; Esserman, L.; Albertson, D. G.; Waldman, F. M.; Gray, J. W. Genomic and transcriptional aberrations linked to breast cancer pathophysiologies. *Cancer Cell* **2006**, *10* (6), 529−41.
(23) Grover-McKay, M.; Walsh, S. A.; Seftor, E. A.; Thomas, P. A.; Hendrix, M. J. Role for glucose transporter 1 protein in human breast cancer. *Pathol. Oncol. Res.* **1998**, *4* (2), 115−20.
(24) Haura, E. B.; Turkson, J.; Jove, R. Mechanisms of disease: Insights into the emerging role of signal transducers and activators of transcription in cancer. *Nat. Clin. Pract. Oncol.* **2005**, *2* (6), 315−24.
(25) Jonsson, M.; Borg, A.; Nilbert, M.; Andersson, T. Involvement of adenomatous polyposis coli (APC)/beta-catenin signalling in human breast cancer. *Eur. J. Cancer* **2000**, *36* (2), 242−8.
(26) Kraemer, F. B.; Shen, W. J. Hormone-sensitive lipase: control of intracellular tri-(di-)acylglycerol and cholesteryl ester hydrolysis. *J. Lipid Res.* **2002**, *43* (10), 1585−94.
(27) Olson, R. E. Discovery of the lipoproteins, their role in fat transport and their significance as risk factors. *J. Nutr.* **1998**, *128* (2 Suppl), 439S−443S.
(28) DeBerardinis, R. J.; Lum, J. J.; Hatzivassiliou, G.; Thompson, C. B. The biology of cancer: metabolic reprogramming fuels cell growth and proliferation. *Cell Metab.* **2008**, *7* (1), 11−20.
(29) Trombetta, E. S.; Mellman, I. Cell biology of antigen processing in vitro and in vivo. *Annu. Rev. Immunol.* **2005**, *23*, 975−1028.
(30) Vesely, M. D.; Kershaw, M. H.; Schreiber, R. D.; Smyth, M. J. Natural innate and adaptive immunity to cancer. *Annu. Rev. Immunol.* **2011**, *29*, 235−71.
(31) Cantor, J.; Browne, C. D.; Ruppert, R.; Feral, C. C.; Fassler, R.; Rickert, R. C.; Ginsberg, M. H. CD98hc facilitates B cell proliferation and adaptive humoral immunity. *Nat. Immunol.* **2009**, *10* (4), 412−9.
(32) Gelderman, K. A.; Tomlinson, S.; Ross, G. D.; Gorter, A. Complement function in mAb-mediated cancer immunotherapy. *Trends Immunol* **2004**, *25* (3), 158−64.
(33) Rutkowski, M. J.; Sughrue, M. E.; Kane, A. J.; Mills, S. A.; Parsa, A. T. Cancer and the complement cascade. *Mol. Cancer Res.* **2010**, *8* (11), 1453−65.
(34) Duggan, D. J.; Bittner, M.; Chen, Y.; Meltzer, P.; Trent, J. M. Expression profiling using cDNA microarrays. *Nat. Genet.* **1999**, *21* (1 Suppl), 10−4.
(35) Hilvo, M.; Denkert, C.; Lehtinen, L.; Muller, B.; Brockmoller, S.; Seppanen-Laakso, T.; Budczies, J.; Bucher, E.; Yetukuri, L.; Castillo, S.; Berg, E.; Nygren, H.; Sysi-Aho, M.; Griffin, J. L.; Fiehn, O.; Loibl, S.; Richter-Ehrenstein, C.; Radke, C.; Hyotylainen, T.; Kallioniemi, O.; Iljin, K.; Oresic, M. Novel theranostic opportunities offered by characterization of altered membrane lipid metabolism in breast cancer progression. *Cancer Res.* **2011**, *71* (9), 3236−45.
(36) Seligson, D. B.; Horvath, S.; Shi, T.; Yu, H.; Tze, S.; Grunstein, M.; Kurdistani, S. K. Global histone modification patterns predict risk of prostate cancer recurrence. *Nature* **2005**, *435* (7046), 1262−6.
(37) Bai, X.; Wu, L.; Liang, T.; Liu, Z.; Li, J.; Li, D.; Xie, H.; Yin, S.; Yu, J.; Lin, Q.; Zheng, S. Overexpression of myocyte enhancer factor 2 and histone hyperacetylation in hepatocellular carcinoma. *J. Cancer Res. Clin. Oncol.* **2008**, *134* (1), 83−91.
(38) Arif, M.; Senapati, P.; Shandilya, J.; Kundu, T. K. Protein lysine acetylation in cellular function and its role in cancer manifestation. *Biochim. Biophys. Acta* **1799**, *10−12*, 702−16.
(39) Dunn, G. P.; Sheehan, K. C.; Old, L. J.; Schreiber, R. D. IFN unresponsiveness in LNCaP cells due to the lack of JAK1 gene expression. *Cancer Res.* **2005**, *65* (8), 3447−53.
(40) Khong, H. T.; Wang, Q. J.; Rosenberg, S. A. Identification of multiple antigens recognized by tumor-infiltrating lymphocytes from a single patient: tumor escape by antigen loss and loss of MHC expression. *J. Immunother.* **2004**, *27* (3), 184−90.
(41) Steinman, R. M.; Hawiger, D.; Nussenzweig, M. C. Tolerogenic dendritic cells. *Annu. Rev. Immunol.* **2003**, *21*, 685−711.
(42) Dhodapkar, M. V.; Steinman, R. M. Antigen-bearing immature dendritic cells induce peptide-specific CD8(+) regulatory T cells in vivo in humans. *Blood* **2002**, *100* (1), 174−7.
(43) Gabrilovich, D. Mechanisms and functional significance of tumour-induced dendritic-cell defects. *Nat. Rev. Immunol.* **2004**, *4* (12), 941−52.
(44) Sakaguchi, S.; Wing, K.; Onishi, Y.; Prieto-Martin, P.; Yamaguchi, T. Regulatory T cells: how do they suppress immune responses? *Int. Immunol.* **2009**, *21* (10), 1105−11.
(45) Kim, S. H.; Carney, D. F.; Hammer, C. H.; Shin, M. L. Nucleated cell killing by complement: effects of C5b-9 channel size and extracellular Ca2+ on the lytic process. *J. Immunol.* **1987**, *138* (5), 1530−6.

(46) Coussens, L. M.; Werb, Z. Inflammation and cancer. *Nature* **2002**, *420* (6917), 860–7.
(47) Bouzahzah, B.; Albanese, C.; Ahmed, F.; Pixley, F.; Lisanti, M. P.; Segall, J. D.; Condeelis, J.; Joyce, D.; Minden, A.; Der, C. J.; Chan, A.; Symons, M.; Pestell, R. G. Rho family GTPases regulate mammary epithelium cell growth and metastasis through distinguishable pathways. *Mol. Med.* **2001**, *7* (12), 816–30.
(48) Bellizzi, A.; Mangia, A.; Chiriatti, A.; Petroni, S.; Quaranta, M.; Schittulli, F.; Malfettone, A.; Cardone, R. A.; Paradiso, A.; Reshkin, S. J. RhoA protein expression in primary breast cancers and matched lymphocytes is associated with progression of the disease. *Int. J. Mol. Med.* **2008**, *22* (1), 25–31.
(49) Jiang, P.; Enomoto, A.; Takahashi, M. Cell biology of the movement of breast cancer cells: intracellular signalling and the actin cytoskeleton. *Cancer Lett.* **2009**, *284* (2), 122–30.
(50) Cichon, M. A.; Degnim, A. C.; Visscher, D. W.; Radisky, D. C. Microenvironmental influences that drive progression from benign breast disease to invasive breast cancer. *J. Mammary Gland Biol. Neoplasia* **2010**, *15* (4), 389–97.
(51) Allinen, M.; Beroukhim, R.; Cai, L.; Brennan, C.; Lahti-Domenici, J.; Huang, H.; Porter, D.; Hu, M.; Chin, L.; Richardson, A.; Schnitt, S.; Sellers, W. R.; Polyak, K. Molecular characterization of the tumor microenvironment in breast cancer. *Cancer Cell* **2004**, *6* (1), 17–32.
(52) Gudjonsson, T.; Ronnov-Jessen, L.; Villadsen, R.; Rank, F.; Bissell, M. J.; Petersen, O. W. Normal and tumor-derived myoepithelial cells differ in their ability to interact with luminal breast epithelial cells for polarity and basement membrane deposition. *J. Cell Sci.* **2002**, *115* (Pt 1), 39–50.
(53) Fenhalls, G.; Geyp, M.; Dent, D. M.; Parker, M. I. Breast tumour cell-induced down-regulation of type I collagen mRNA in fibroblasts. *Br. J. Cancer* **1999**, *81* (7), 1142–9.